Available online at www.sciencedirect.com
ScienceDirect
Journal of Sound and Vibration 301 (2007) 878–897
JOURNAL OF SOUND AND VIBRATION
www.elsevier.com/locate/jsvi

A lumped-mass TMM for free vibration analysis of a multi-step Timoshenko beam carrying eccentric lumped masses with rotary inertias

Jong-Shyong Wu*, Chin-Tzu Chen

Department of Naval Architecture and Marine Engineering, National Cheng-Kung University, Tainan 701, Taiwan, ROC

Received 23 January 2006; received in revised form 5 September 2006; accepted 28 October 2006
Available online 22 December 2006

Abstract

In the conventional lumped-mass (model) transfer matrix method (LTMM), one must use different frequency equation and the associated initial parameters to determine the natural frequencies and the corresponding mode shapes of a beam with different boundary (supporting) conditions as one may see from the *Appendix* at the end of this paper. Besides, the eccentricity of each attached lumped mass is also neglected in the existing LTMM. The purpose of this paper is to present a modified LTMM so that one may easily determine the natural frequencies and the corresponding mode shapes of a multi-step Timoshenko beam with various boundary (supporting) conditions and carrying various concentrated elements with eccentricity of each lumped mass considered, by using the same formulation developed from a beam with ''free–free'' boundary conditions.To this end, by considering the effect of rotary inertia of each beam segment and the eccentricity of each attached lumped mass, the transfer matrix for a typical *station* carrying three kinds of concentrated elements is derived. Meanwhile, by considering the shear deformation of each beam segment, the transfer matrix for a typical *field* is also deduced. It has been found that, by changing the magnitude (from zero to infinity) of each concentrated element, one may easily model many problems studied in the exiting literature concerned. The reliability of the presented approach has been confirmed by the good agreement between the numerical results of this paper and those of the existing literature or the conventional finite element method (FEM).

1. Introduction

Since the dynamic characteristics of some structural systems may be predicted by using a beam carrying single or multiple concentrated elements, the literature concerned is plenty. For the free vibration analysis of beams with various attachments, the lumped-mass (model) transfer matrix method (LTMM) was one of the most popular approaches in early years [1–4]. Later, various classical analytical methods were also presented [5–12]. In the last two decades, some researchers further devoted themselves to the study of continuous-mass (model) transfer matrix method (CTMM) to improve the accuracy of the LTMM [13–15].

*Corresponding author.
E-mail address: jswu@mail.ncku.edu.tw (J.-S. Wu).

0022-460X/$ - see front matter © 2006 Elsevier Ltd. All rights reserved.
doi:10.1016/j.jsv.2006.10.022

From the existing literature concerning LTMM [4], one finds that the frequency equation and the associated initial state variables (or initial parameters) required for the determination of natural frequencies and corresponding mode shapes of a beam must be changed case by case according to its various boundary (supporting) conditions. To improve the last drawback of the existing LTMM, this paper presents the modified transfer matrices for each *station* and each *field* of a "free–free" beam. In which, in addition to the conventional lumped mass $m_{b,i}$ and rotary inertia $J_{b,i}$ due to each beam segment, three kinds of attachments including a lumped mass $m_{a,i}$ (with rotary inertia $J_{a,i}$ and eccentricity e_i), a translational spring (with stiffness constant $k_{t,i}$) and a rotational spring (with stiffness constant $k_{r,i}$) are also attached to each *station*. Besides, by considering the effect of shear deformation of each beam segment, the transfer matrix for each *field* is deduced. In such way, one may easily model the free end of a beam by setting $k_{t,i} = 0$ and $k_{r,i} = 0$, the pinned end of a beam by setting $k_{t,i} \approx \infty$ and $k_{r,i} = 0$, and the clamped end of a beam by setting $k_{t,i} \approx \infty$ and $k_{r,i} = \infty$, where i denotes the station numbering. Since the last formulation based on the theory developed from a "free–free" beam carrying a number of concentrated elements is available for the beams with various boundary conditions, use of the frequency equations and the associated initial parameters for various boundary conditions required by the conventional LTMM (cf. *Appendix* of this paper) is not necessary. It is evident that one may easily establish the mathematical model of a multi-step Timoshenko beam with various boundary conditions carrying any sets of attachments by only changing the magnitudes of the relevant elements ($m_{a,i}, J_{a,i}, e_i, k_{t,i}$ and/or $k_{r,i}$) attached to each *station* and the cross-sectional area together with the length of each beam segment associated with each *field*.

For convenience, the LTMM based on the theory of this paper is called LTMM1 and that based on the classical (existing) approach is called LTMM0. To confirm the reliability of the presented theory, the lowest five natural frequencies and/or the corresponding mode shapes of the uniform and non-uniform (multi-step) beams with various classical and/or non-classical boundary conditions are determined. Good agreements between the numerical results of LTMM1, LTMM0, the existing analytical methods and/or the conventional FEM have been achieved.

Compared with FEM, the transfer matrix method (TMM) has the following advantages: (i) In this paper, the order of transfer matrix for each field or station is 4×4, therefore, the order of *overall transfer matrix* for the entire beam is always 4×4 no matter how many fields or stations composing of the entire beam; however, this is not true for FEM. For each two-node beam element studied in this paper, each beam element has 4 degrees of freedom (dof's), therefore, before considering the boundary conditions, the order of *overall mass matrix* (or *overall stiffness matrix*) of the entire beam is $2(n+1) \times 2(n+1)$ with n denoting the total number of beam elements. For the last reasons, the computing speed of FEM will "significantly" decrease with the increase of total number of beam elements (n), but that of TMM only "silghtly" decreases with the increase of n. (ii) The state variables for FEM are displacements, velocities and accelerations, but those of TMM are displacements, slopes, bending moments and shearing forces. For some problems like that studied in Ref. [16], in addition to the mode "displacements" the associated mode "bending moments" (or "curvaures") of the entire beam are also required; in such a case, the TMM will be more effective than FEM. (iii) In general, TMM is used for the "free" vibration analysis; however, incorporated with the mode superposition method, TMM can also provide a simple approach for the "forced" vibration analysis of beams subjected to moving loads as one may see from Ref. [17]. On the other hand, for the title problem, the presented TMM may be one of the simplest tools for checking the correctness of the FEM results.

2. Transfer matrices of a station, a field and a section

For the LTMM, a continuous beam must be replaced by a number of lumped masses $m_{b,i}$ ($i = 1$ to $n+1$) connected by a number of massless uniform beam segments with lengths ℓ_i. The positions occupied by the lumped masses are called *stations* and the massless uniform beam segments responsible for the bending stiffness of the entire beam are called *fields*. For convenience, a station together with a field is called a *section* [3,4] as shown in Fig. 1(a), in which, e_i denotes the eccentricity of the "attached" lumped mass $m_{a,i}$ with rotary inertia $J_{a,i}$ located at station i, and $m_i = m_{a,i} + m_{b,1}$ and $J_i = J_{a,i} + J_{b,1}$ with subscripts a and b referring to *attachment* and *beam* segment, respectively, while E_i, G_i, A_i and I_i denote the Young's modulus, shear modulus, cross-sectional area and area moment of inertia of the beam segment for field (i), respectively.

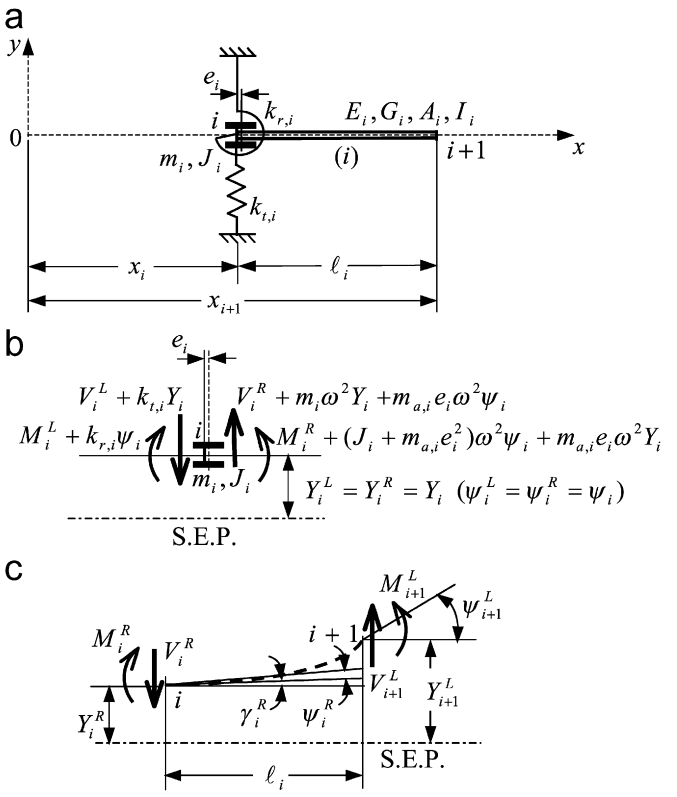

Fig. 1. (a) *Section i* is comprised of *station i* and *field* (*i*); (b) free-body diagram of *station i*; (c) free-body diagram of *field* (*i*). Where $m_i = m_{a,i} + m_{b,1}$ and $J_i = J_{a,i} + J_{b,1}$ with subscripts *a* and *b* referring to *attachment* and *beam* segment, respectively.

In addition to the above-mentioned lumped mass m_i and rotary inertia J_i, a translational spring with stiffness constant $k_{t,i}$ and a rotational spring with stiffness constant $k_{r,i}$ are also attached to station i. Since the location of station i is defined by $x = x_i$, the length of field (i) is given by $\ell_i = x_{i+1} - x_i$. The free-body diagrams for station i and field (i) are shown in Figs. 1(b) and (c), respectively, with SEP referring to the static equilibrium position of the un-deformed beam.

2.1. Transfer matrix of a station

From the free-body diagram for station i shown in Fig. 1(b), one has

$$Y_i^R = Y_i^L = Y_i, \tag{1}$$

$$\psi_i^R = \psi_i^L = \psi_i, \tag{2}$$

$$M_i^R = M_i^L - m_{a,i}e_i\omega^2 Y_i^L + [k_{r,i} - (J_i + m_{a,i}e_i^2)\omega^2]\psi_i^L, \tag{3}$$

$$V_i^R = V_i^L + (k_{t,i} - m_i\omega^2)Y_i^L - m_{a,i}e_i\omega^2\psi_i^L, \tag{4}$$

where Y_i^L, ψ_i^L, M_i^L and V_i^L denote the transverse displacement, slope, bending moment and shearing force at the "left" side of station i, respectively, while Y_i^R, ψ_i^R, M_i^R and V_i^R denote the same quantities at the "right" side of station i, respectively. It is evident that, Eqs. (1) and (2) denote the continuities of displacements and slopes at station i, while Eqs. (3) and (4) denote the equilibriums of the bending moments and shear forces at the "left" side and the "right" side of station i, respectively. Since ω denotes the natural frequency of the entire beam, all terms containing ω^2 in Fig. 1(b) and Eqs. (3) and (4) denote the inertia forces induced by the lumped

mass m_i (or $m_{a,i}$) or inertia bending moment induced by the rotary inertia J_i (or the lumped mass $m_{a,i}$ and its eccentricity e_i).

To write Eqs. (1)–(4) in matrix form gives

$$\{\delta\}_i^R = [T_S]_i\{\delta\}_i^L, \tag{5}$$

where

$$\{\delta\}_i^R = \{Y_i^R\ \psi_i^R\ M_i^R\ V_i^R\}, \tag{6a}$$

$$\{\delta\}_i^L = \{Y_i^L\ \psi_i^L\ M_i^L\ V_i^L\}, \tag{6b}$$

$$[T_S]_i = \left[\begin{array}{cc:cc} 1 & 0 & 0 & 0 \\ 0 & 1 & 0 & 0 \\ \hdashline -m_{a,i}e_i\omega^2 & k_{r,i} - (J_i + m_{a,i}e_i^2)\omega^2 & 1 & 0 \\ k_{t,i} - m_i\omega^2 & -m_{a,i}e_i\omega^2 & 0 & 1 \end{array}\right]. \tag{7}$$

In the last expressions, the symbol $\{\cdot\}$ denotes a column vector and $[T_S]_i$ is the transfer matrix of station i. Note that the eccentricity e_i of the lumped mass $m_{a,i}$ is not considered in the existing literature [1–4], besides, the lumped mass m_i and the rotary inertia J_i are determined as follows:

$$m_i = m_{a,i} + m_{b,i}, \tag{8}$$

where $m_{a,i}$ is the "attached" lumped mass at station i and $m_{b,i}$ is the lumped mass at station i due to the "beam" segments connected to station i. If ρ_i denotes the mass density of beam segment (i), then one has

$$m_{b,1} = \tfrac{1}{2}\rho_1 A_1 \ell_1 \quad \text{(for station 1)}, \tag{9a}$$

$$m_{b,n+1} = \tfrac{1}{2}\rho_n A_n \ell_n \quad \text{(for final station } n+1), \tag{9b}$$

$$m_{bi} = \tfrac{1}{2}(\rho_{i-1}A_{i-1}\ell_{i-1} + \rho_i A_i \ell_i) \quad \text{(for each intermediate station } i). \tag{9c}$$

Similarly, one has

$$J_i = J_{a,i} + J_{b,i} \tag{10}$$

with

$$J_{b,1} = \tfrac{1}{2}\rho_1 I_1 \ell_1 \quad \text{(for station 1)}, \tag{11a}$$

$$J_{b,n+1} = \tfrac{1}{2}\rho_n I_n \ell_n \quad \text{(for final station } n+1), \tag{11b}$$

$$J_{b,i} = \tfrac{1}{2}(\rho_{i-1}I_{i-1}\ell_{i-1} + \rho_i I_i \ell_i) \quad \text{(for each intermediate station } i), \tag{11c}$$

where $J_{a,i}$ is rotary inertia at station i due to the "attachment" and $J_{b,i}$ is the rotary inertia at station i due to the "beam" segments connected to station i. If the rotary inertia is neglected (such as the case for a Euler–Bernoulli beam), then $J_{b,i} = 0$ ($i = 1$ to $n+1$), with $n+1$ denoting the total number of stations.

2.2. Transfer matrix of a field

From the free-body diagram for field (i) shown in Fig. 1(c), one has

$$V_{i+1}^L = V_i^R, \tag{12}$$

$$M_{i+1}^L = M_i^R - \ell_i V_{i+1}^L, \tag{13}$$

$$\psi_{i+1}^{L} = \psi_i^R + a_i^{\psi M} M_{i+1}^{L} + a_i^{\psi V} V_{i+1}^{L}, \tag{14}$$

$$Y_{i+1}^{L} = Y_i^R + (\psi_i^R + \gamma_i^R)\ell_i + a_i^{YM} M_{i+1}^{L} + a_i^{YV} V_{i+1}^{L}, \tag{15}$$

where the symbols a_i^{YM} and $a_i^{\psi M}$, respectively, denote the linear and angular displacements at station $i+1$ relative to station i due to action of a unit bending moment at station $i+1$ (i.e., $M_{i+1}^{L}=1$); similarly, the symbols a_i^{YV} and $a_i^{\psi V}$, respectively, denote those due to action of a unit force at station $i+1$ (i.e., $V_{i+1}^{L}=1$). From the textbook regarding the strength of material [18], one has

$$a_i^{YM} = \frac{\ell_i^2}{2E_iI_i}, \quad a_i^{\psi M} = \frac{\ell_i}{E_iI_i}, \tag{16a,b}$$

$$a_i^{YV} = \frac{\ell_i^3}{3E_iI_i}, \quad a_i^{\psi V} = \frac{\ell_i^2}{2E_iI_i}. \tag{17a,b}$$

The symbol γ_i^R in Eq. (15) denotes the shear deformation (or strain) at the right side of station i due to shear force V_i^R, i.e.,

$$\gamma_i^R = \frac{V_i^R}{k_i' G_i A_i}, \tag{18}$$

where k_i' and G_i are shear correction factor and shear modulus of the beam segment for field (i), respectively. Since the shear force throughout the field (i) is constant so is the shear deformation γ_i^R ($=\gamma_i^L=\gamma_i$). If the shear deformation is neglected (such as the case for a Euler–Bernoulli beam), then $\gamma_i^R=\gamma_i^L=\gamma_i=0$.

Substituting Eq. (12) into Eq. (13) gives

$$M_{i+1}^{L} = M_i^R - \ell_i V_i^R. \tag{13$'$}$$

Introducing the relationships given by Eqs. (12), (13)′, (16)–(18) into Eqs. (14) and (15), one obtains

$$\psi_{i+1}^{L} = \psi_i^R + \left(\frac{\ell_i}{E_iI_i}\right) M_i^R - \left(\frac{\ell_i^2}{2E_iI_i}\right) V_i^R, \tag{14$'$}$$

$$Y_{i+1}^{L} = Y_i^R + \ell_i\psi_i^R + \left(\frac{\ell_i^2}{2E_iI_i}\right) M_i^R - \left(\frac{\ell_i^3}{6E_iI_i} - \frac{\ell_i}{k_i' G_i A_i}\right) V_i^R. \tag{15$'$}$$

To write Eqs. (15)′, (14)′, (13)′ and (12) in matrix form yields

$$\{\delta\}_{i+1}^{L} = [T_F]_i \{\delta\}_i^R \tag{19}$$

with

$$\{\delta\}_{i+1}^{L} = \{Y_{i+1}^{L}\ \psi_{i+1}^{L}\ M_{i+1}^{L}\ V_{i+1}^{L}\}, \tag{20a}$$

$$\{\delta\}_i^R = \{Y_i^R\ \psi_i^R\ M_i^R\ V_i^R\}, \tag{20b}$$

$$[T_F]_i = \left[\begin{array}{cc:cc} 1 & \ell_i & \dfrac{\ell_i^2}{2E_iI_i} & -\left(\dfrac{\ell_i^3}{6E_iI_i} - \dfrac{\ell_i}{k_i' G_i A_i}\right) \\ 0 & 1 & \dfrac{\ell_i}{E_iI_i} & -\dfrac{\ell_i^2}{2E_iI_i} \\ \hdashline 0 & 0 & 1 & -\ell_i \\ 0 & 0 & 0 & 1 \end{array}\right]. \tag{21}$$

This is the transfer matrix for field (i). It is noted that $\ell_{n+1}=0$ with n denoting the total number of *fields* and $n+1$ the total number of *stations*.

2.3. Transfer matrix of a section

From Eqs. (5) and (19) one obtains

$$\{\delta\}_{i+1}^{L}=[T_F]_i[T_S]_i\{\delta\}_i^{L}=[T]_i\{\delta\}_i^{L}, \tag{22}$$

where

$$\{\delta\}_{i+1}^{L}=\{Y_{i+1}^{L}\ \psi_{i+1}^{L}\ M_{i+1}^{L}\ V_{i+1}^{L}\}, \tag{23a}$$

$$\{\delta\}_{i}^{L}=\{Y_{i}^{L}\ \psi_{i}^{L}\ M_{i}^{L}\ V_{i}^{L}\}, \tag{23b}$$

$$[T]_i=[T_F]_i[T_S]_i=\left[\begin{array}{cc:cc} T_{11} & T_{12} & \dfrac{\ell_i^2}{2E_iI_i} & -\left(\dfrac{\ell_i^3}{6E_iI_i}-\dfrac{\ell_i}{k_i'G_iA_i}\right)\\ T_{21} & T_{22} & \dfrac{\ell_i}{E_iI_i} & -\dfrac{\ell_i^2}{2E_iI_i}\\ \hdashline T_{31} & T_{32} & 1 & -\ell_i\\ k_{t,i}-m_i\omega^2 & \underline{-m_{a,i}e_i\omega^2} & 0 & 1 \end{array}\right] \tag{24}$$

with

$$T_{11}=1-\left(\frac{\ell_i^3}{6E_iI_i}-\frac{\ell_i}{k_i'G_iA_i}\right)(k_{t,i}-m_i\omega^2)-\underline{\frac{\ell_i^2(m_{a,i}e_i\omega^2)}{2E_iI_i}}, \tag{25a}$$

$$T_{12}=\ell_i+\frac{\ell_i^2}{2E_iI_i}[k_{r,i}-(J_i+\underline{m_{a,i}e_i^2})\omega^2]+\left(\underline{\frac{\ell_i^3}{6E_iI_i}}-\underline{\frac{\ell_i}{k_i'G_iA_i}}\right)(m_{a,i}e_i\omega^2), \tag{25b}$$

$$T_{21}=-\frac{\ell_i^2}{2E_iI_i}(k_{t,i}-m_i\omega^2)-\underline{\frac{\ell_i(m_{a,i}e_i\omega^2)}{E_iI_i}}, \tag{25c}$$

$$T_{22}=1+\frac{\ell_i}{E_iI_i}[k_{r,i}-(J_i+\underline{m_{a,i}e_i^2})\omega^2]+\underline{\frac{\ell_i^2(m_{a,i}e_i\omega^2)}{2E_iI_i}}, \tag{25d}$$

$$T_{31}=-[\ell_i(k_{t,i}-m_i\omega^2)+\underline{(m_{a,i}e_i\omega^2}], \tag{25e}$$

$$T_{32}=k_{r,i}-(J_i+\underline{m_{a,i}e_i^2})\omega^2+\underline{\ell_i(m_{a,i}e_i\omega^2)}. \tag{25f}$$

The matrix $[T]_i$ defined by Eq. (24) denotes the transfer matrix of section i. From Eq. (22) one sees that the state variables at the "left" side of station $i+1$, $\{\delta\}_{i+1}^{L}=\{Y_{i+1}^{L}\ \psi_{i+1}^{L}\ M_{i+1}^{L}\ V_{i+1}^{L}\}$, may be obtained from those at the "left" side of station i, $\{\delta\}_i^{L}=\{Y_i^{L}\ \psi_i^{L}\ M_i^{L}\ V_i^{L}\}$, by using the transfer matrix of section i, $[T]_i$, given by Eq. (24).

It is noted that the underlined terms in Eqs. (24) and (25) are due to the eccentricity e_i of the attached lumped mass at station i, $m_{a,i}$, they are not considered in the existing LTMM [1–4]. Thus, if these terms are neglected, one obtains the following classical transfer matrix of section i for the

Timoshenko beam

$$[T]_i = \left[\begin{array}{cc:cc} 1-\left(\frac{\ell_i^3}{6E_iI_i}-\frac{\ell_i}{k_i'G_iA_i}\right)\left(k_{t,i}-m_i\omega^2\right) & \ell_i+\frac{\ell_i^2}{2E_iI_i}\left(k_{r,i}-J_i\omega^2\right) & \frac{\ell_i^2}{2E_iI_i} & -\left(\frac{\ell_i^3}{6E_iI_i}-\frac{\ell_i}{k_i'G_iA_i}\right) \\ -\frac{\ell_i^2}{2E_iI_i}\left(k_{t,i}-m_i\omega^2\right) & 1+\frac{\ell_i}{E_iI_i}\left(k_{r,i}-J_i\omega^2\right) & \frac{\ell_i}{E_iI_i} & -\frac{\ell_i^2}{2E_iI_i} \\ \hdashline -\ell_i\left(k_{t,i}-m_i\omega^2\right) & k_{r,i}-J_i\omega^2 & 1 & -\ell_i \\ k_{t,i}-m_i\omega^2 & 0 & 0 & 1 \end{array}\right]. \tag{24'}$$

In practice, one may set $m_{a,i}=0$, $J_{a,i}=0$, $e_i=0$, $k_{t,i}=0$ and/or $k_{r,i}=0$ according to the actual situations. For example, one may set $m_{a,i}=J_{a,i}=e_i=k_{t,i}=k_{r,i}=0$ for a station without any attachments; $e_i=k_{t,i}=k_{r,i}=0$ for a station carrying only an "attached" lumped mass $m_{a,i}$ possessing rotary inertia $J_{a,i}$ but without eccentricity; $m_{a,i}=J_{a,i}=e_i=k_{r,i}=0$ for a station supported by a translational spring with stiffness constant $k_{t,i}$; etc.

3. Determination of natural frequencies and mode shapes

Repeated application of Eq. (22) yields the following relationships:

$$\{\delta\}_2^L=[T]_1\{\delta\}_1^L \tag{26a}$$

$$\{\delta\}_3^L=[T]_2\{\delta\}_2^L=[T]_2[T]_1\{\delta\}_1^L \tag{26b}$$

$$\{\delta\}_4^L=[T]_3\{\delta\}_3^L=[T]_3[T]_2[T]_1\{\delta\}_1^L \tag{26c}$$

$$\cdots\cdots\cdots$$

$$\{\delta\}_{n+1}^L=[T]_n\{\delta\}_n^L=[T]_n\ldots[T]_3[T]_2[T]_1\{\delta\}_1^L \tag{26d}$$

$$\{\delta\}_{n+1}^R=[T_S]_{n+1}\{\delta\}_{n+1}^L=[T_S]_{n+1}[T]_n\ldots[T]_3[T]_2[T]_1\{\delta\}_1^L=[\overline{T}]\{\delta\}_1^L \tag{26e}$$

with

$$[\overline{T}]=[T_S]_{n+1}[T]_n\ldots[T]_3[T]_2[T]_1=\begin{bmatrix}\overline{T}_{11} & \overline{T}_{12} & \overline{T}_{13} & \overline{T}_{14}\\ \overline{T}_{21} & \overline{T}_{22} & \overline{T}_{23} & \overline{T}_{24}\\ \overline{T}_{31} & \overline{T}_{32} & \overline{T}_{33} & \overline{T}_{34}\\ \overline{T}_{41} & \overline{T}_{42} & \overline{T}_{43} & \overline{T}_{44}\end{bmatrix}. \tag{27}$$

In Eqs. (26e) and (27), $[T_S]_{n+1}$ denotes the transfer matrix of the final *station* $n+1$ and may be determined from Eq. (7) by setting $i=n+1$. However, one may also determine the value of $[T_S]_{n+1}$ from the transfer matrix of a *section* defined by Eqs. (24) and (25) by setting $i=n+1$ and $\ell_i=\ell_{n+1}=0$ as mentioned next Eq. (21).

The symbol $[\overline{T}]$ in Eq. (26e) or (27) denotes the "overall" transfer matrix for the entire beam. It is a 4×4 square matrix. From Eq. (26e) one obtains the relationships between the state variables at the "left side" of the beam, $\{\delta\}_1^L=\{Y_1^L\ \psi_1^L\ M_1^L\ V_1^L\}$, and those at the "right side" of the beam, $\{\delta\}_{n+1}^R=\{Y_{n+1}^R\ \psi_{n+1}^R\ M_{n+1}^R\ V_{n+1}^R\}$, to take the form

$$Y_{n+1}^R=\overline{T}_{11}Y_1^L+\overline{T}_{12}\psi_1^L+\overline{T}_{13}M_1^L+\overline{T}_{14}V_1^L, \tag{28a}$$

$$\psi_{n+1}^R=\overline{T}_{21}Y_1^L+\overline{T}_{22}\psi_1^L+\overline{T}_{23}M_1^L+\overline{T}_{24}V_1^L, \tag{28b}$$

$$M_{n+1}^R = \overline{T}_{31} Y_1^L + \overline{T}_{32}\psi_1^L + \overline{T}_{33} M_1^L + \overline{T}_{34} V_1^L, \tag{28c}$$

$$V_{n+1}^R = \overline{T}_{41} Y_1^L + \overline{T}_{42}\psi_1^L + \overline{T}_{43} M_1^L + \overline{T}_{44} V_1^L. \tag{28d}$$

For a "free–free" beam carrying any sets of concentrated elements, the bending moment and shearing force at its "left side", M_1^L and V_1^L, and those at its "right side", M_{n+1}^R and V_{n+1}^R are equal to zero, i.e.,

$$M_1^L = 0, \quad V_1^L = 0, \tag{29a,b}$$

$$M_{n+1}^R = 0, \quad V_{n+1}^R = 0. \tag{30a,b}$$

The substitutions of Eqs. (29) and (30) into Eqs. (28c) and (28d), respectively, lead to

$$\overline{T}_{31} Y_1^L + \overline{T}_{32}\psi_1^L = 0, \tag{31a}$$

$$\overline{T}_{41} Y_1^L + \overline{T}_{42}\psi_1^L = 0. \tag{31b}$$

Non-trivial solution for Eqs. (31a) and (31b) requires that

$$\Delta(\omega) = \begin{vmatrix} \overline{T}_{31} & \overline{T}_{32} \\ \overline{T}_{41} & \overline{T}_{42} \end{vmatrix} = 0. \tag{32}$$

Eq. (32) is the frequency equation of a "free–free" beam, from which one may determine the natural frequencies of the beam. Corresponding to each natural frequency ω_v one may obtain the corresponding mode shape $\{Y\}_v = \{Y_1\ Y_2\ \cdots\ Y_{n+1}\}_v$ from Eq. (26a)–(26e), if the initial state variables $\{\delta\}_0$ are given. For a "free–free" beam, the initial state variables (or initial parameters) are given by

$$\{\delta\}_0 = \begin{Bmatrix} Y_0 \\ \psi_0 \\ M_0 \\ V_0 \end{Bmatrix} = \begin{Bmatrix} Y_1^L \\ \psi_1^L \\ M_1^L \\ V_1^L \end{Bmatrix} = \begin{Bmatrix} 1 \\ -\overline{T}_{31}/\overline{T}_{32} \\ 0 \\ 0 \end{Bmatrix}. \tag{33}$$

In Eq. (33), the values of M_1^L and V_1^L are given by Eq. (29), while those of Y_1^L and ψ_1^L are determined from Eq. (31a) by setting $Y_1^L = 1$.

Although the above formulation given by Eqs. (29)–(33) are obtained from a "free–free" beam carrying a number of concentrated elements, it is also available for the beams with *various* boundary (supporting) conditions as one may see from the next section "Numerical results and discussions". This is because one may obtain *various* boundary conditions by only adjusting the magnitudes of the stiffness constants of the boundary translational spring and/or rotational spring supporting a "free–free" beam. However, according to the existing LTMM [1–4], the natural frequencies and the corresponding mode shapes of a beam with different boundary conditions are determined from different frequency equations together with different initial state variables (or initial parameters) as one may see from the *Appendix* at the end of this paper. According to the foregoing descriptions, it is easy to see the advantage of the modified LTMM presented in this paper.

For convenience, the LTMM based on the above formulation deduced from the theory of a "free–free" beam given by Eqs. (29)–(33) is called LTMM1 and the LTMM based on the classical formulation with *various* frequency equations together with the associated initial parameters for *various* boundary (supporting) conditions shown in the *Appendix* of this paper is called LTMM0, hereafter.

4. Numerical results and discussion

Unless particularly mentioned, the numerical results of this paper are obtained based on the following physical quantities of the uniform beam: total length $L = 2.0\,\text{m}$, diameter $d_1 = 0.03\,\text{m}$, mass density $\rho_1 = 7850\,\text{kg/m}^3$ Young's modulus $E_1 = 2.068 \times 10^{11}\,\text{N/m}^2$, cross-sectional area $A_1 = \pi d_1^2/4 = 7.069 \times 10^{-4}\,\text{m}^2$, area moment of inertia $I_1 = \pi d_1^4/64 = 3.976 \times 10^{-8}\,\text{m}^4$, reference mass $\tilde{m} = \rho_1 A_1 L = 11.09833\,\text{kg}$, reference rotary inertia $\tilde{J} = \rho_1 A_1 L^3 = \tilde{m}L^2 = 44.39332\,\text{kg m}^2$, reference rigidity $E_1 I_1 = 8.2224 \times 10^3\,\text{N m}^2$, reference

rotational spring constant $\tilde{k}_r = E_1 I_1/L = 4.1112 \times 10^3$ N m, reference translational spring constant $\tilde{k}_t = E_1 I_1/L^3 = 1.0278 \times 10^3$ N/m. In the foregoing expressions, the subscript 1 refers to *field* 1 (or *beam segment* 1).

4.1. Validation of the presented theory and the developed computer program

In addition to comparing with the exact solutions of the uniform beams without any attachments (i.e., $m_{a,i} = J_{a,i} = e_i = k_{t,i} = k_{r,i} = 0$ for $i = 1$ to $n+1$) in various classical boundary conditions (BCs), in this subsection, the results of LTMM1 are also compared with the available ones of the beams carrying various concentrated elements in the non-classical boundary conditions (BCs).

4.1.1. A uniform beam without attachments

For a uniform Euler–Bernoulli beam with dimensions and physical properties as shown at the beginning of the current section, its lowest five non-dimensional frequency coefficients, $\beta_v L = \sqrt[4]{\omega_v^2 . \rho_1 A_1 L^4/(E_1 I_1)}$ ($v = 1$–5), are listed in Table 1. In which, P–P, C–C and C–F denote the pinned–pinned, clamped–clamped and clamped–free beams, respectively, with P, C, F representing the abbreviatons of "pinned", "clamped" and "free" respectvely Besides, the "Exact" values refer to the exact solutons for the non-dimensional frequency coefficients $\beta_v L$ given by Ref. [19]. Since the total number of "stations" used throughout this paper is $n+1 = 41$, the total number of "fields" is $n = 40$ with identical length for each beam segment $\ell_i = L/n = 2/40 = 0.05$ m ($i = 1$–40) and $\ell_{41} = 0$. For the results of LTMM1, a P–P beam is obtained from a "free–free" beam carrying $n+1$ sets of concentrated attachments by setting all the attachments to be equal to zero except the stiffness constants at the left end (station 1) and the right end (station 41) of the beam: $k_{t,1} = 1.0 \times 10^{15}$, $k_{r,1} = 0$, $k_{t,41} = 1.0 \times 10^{15}$ and $k_{r,41} = 0$, with unit of $k_{t,i}$ being N/m and that of $k_{r,i}$ being N m ($i = 1$–41). Similarly, the C–C and C–F beams are obtained from the above-mentoned "free–free" beam by setting: ($k_{t,1} = k_{r,1} = k_{t,41} = k_{r,41} = 1.0 \times 10^{15}$) and ($k_{t,1} = k_{r,1} = 1.0 \times 10^{15}$ and $k_{t,41} = k_{r,41} = 0$), respectively. However, the results of LTMM0 are obtained based on the actual boundary conditions of a beam without any attachment and the associated frequency equations together with the initial parameters given in *Appendix* of this paper for the P–P, C–C and C–F beams, respectively. From Table 1, one sees that the non-dimensional frequency coefficients obtained from LTMM1 are very close to the corresponding ones obtained from LTMM0, besides, the agreement between the results of LTMM1 (or LTMM0) and the exact ones [19] is excellent. Fig. 2(a) and (b) shows the lowest five mode shapes of the P–P and C–C beams, respectively. Where the curves with symbols •, +, ▲, ■ and ⋆ represent the 1st, 2nd, 3rd, 4th and 5th mode shapes obtained from LTMM1 (or LTMM0), respectively, while those with symbols ○, ×, △, □ and ☆ present the corresponding

Table 1

The lowest five non-dimensional frequency coefficients, $\beta_v L = \sqrt[4]{\omega_v^2 \cdot \rho_1 A_1 L^4/(E_1 I_1)}$ ($v = 1$–5), for a Euler–Bernoulli beam obtained from presented LTMM1, classical LTMM0 and exact solutions

Boundary conditions	Methods	Non-dimensional frequency coefficients				
		$\beta_1 L$	$\beta_2 L$	$\beta_3 L$	$\beta_4 L$	$\beta_5 L$
P–P	LTMM1[a]	3.1416	6.2832	9.4248	12.5664	15.7080
	LTMM0[a]	3.1416	6.2832	9.4248	12.5664	15.7080
	Exact [17]	3.1416	6.2832	9.4248	12.5664	15.7080
C–C	LTMM1	4.7300	7.8532	10.9956	14.1372	17.2787
	LTMM0	4.7300	7.8532	10.9956	14.1372	17.2787
	Exact [17]	4.7300	7.8532	10.9956	14.1372	17.2788
C–F	LTMM1	1.8750	4.6935	7.8532	10.9924	14.1320
	LTMM0	1.8750	4.6935	7.8532	10.9924	14.1320
	Exact [17]	1.8751	4.6941	7.8548	10.9955	14.1372

[a]Total number of beam segments (or fields) is $n = 40$.

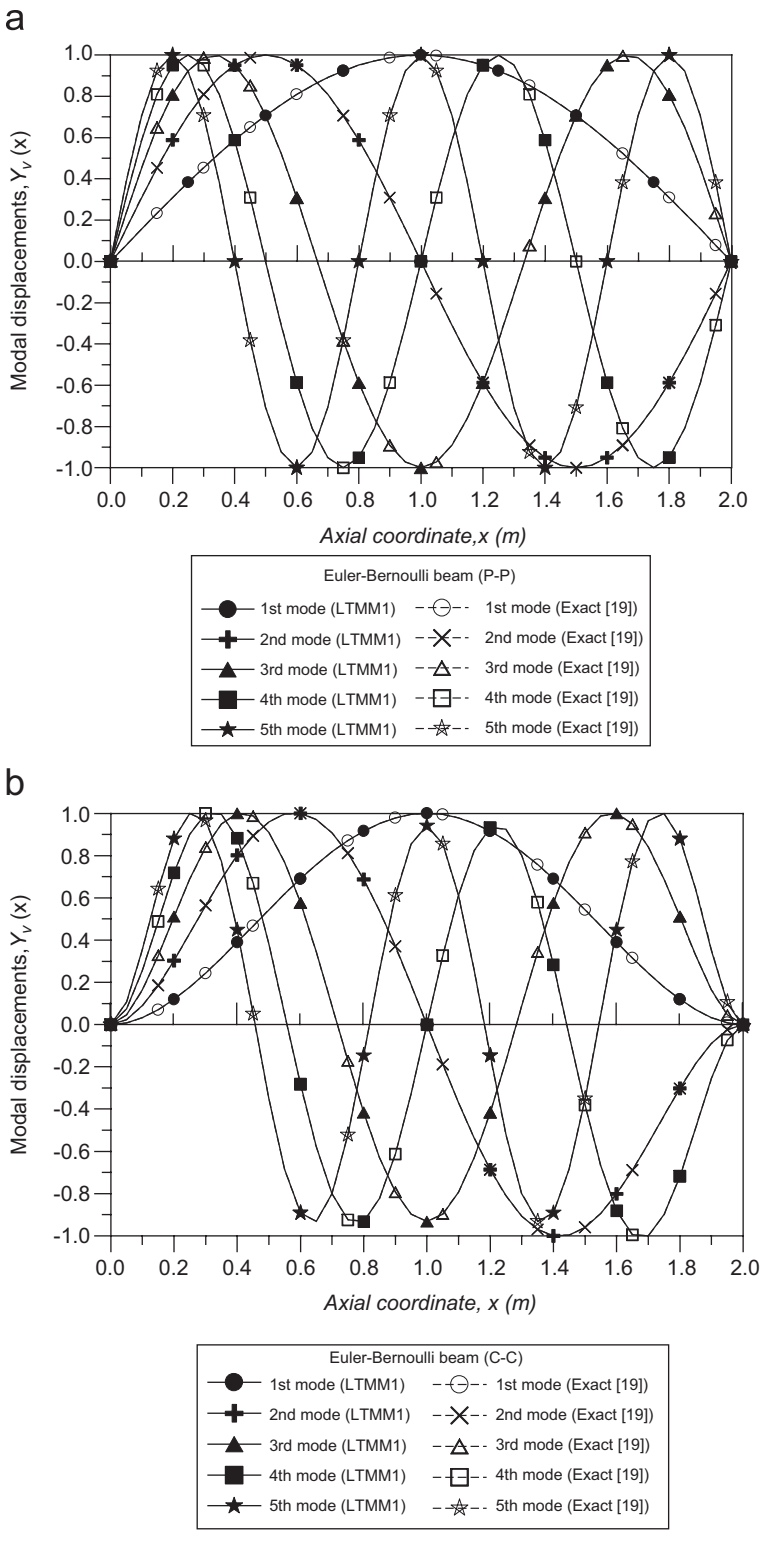

Fig. 2. The lowest five mode shapes of the uniform *Euler–Bernoulli beam* corresponding to the frequency coefficients ($\beta_v L$) listed in Table 1: (a) P–P beam; (b) C–C beam: —●—, —+—, —▲—, —■—, —★— obtained from LTMM1; ---○---, ---×---, ---△---, ---□---, ---☆--- obtained from exact solutions [19].

mode shapes obtained from the exact solutions [19]. It is evident that the lowest five mode shapes of the P–P and C–C beams obtained from LTMM1 (or LTMM0) are very close to the corresponding ones obtained from the exact solutions. This is under expectation, because the lowest five non-dimensional frequency coefficients of the P–P and C–C beams obtained from LTMM1 (or LTMM0) are very close to those obtained from the exact solutions as shown in Table 1.

The next example studied is a uniform Timoshenko beam with dimensions and physical properties given by [20]: total length $L = 40\,\text{in}$, Young's modulus $E = 30 \times 10^6\,\text{psi}$, shear modulus $G = 11.538 \times 10^6\,\text{psi}$ (or Poisons ratio $v = 0.3$), cross-sectional area $A = 2.0 \times 6.9282 = 13.856406\,\text{in}^2$, area moment of inertia $I = 55.42562\,\text{in}^4$, mass density of beam material $\rho = 0.283\,\text{lb}_m/\text{in}^3$, mass per unit length $m' = \rho A = 3.9213629\,\text{lb}_m$, radius of gyration $r_g = \sqrt{I/A} = 2.0\,\text{in}$, shear coefficient (or shape factor) $k' = 5/6$ and total mass of the beam $\tilde{m} = \rho AL = 156.8545159\,\text{lb}_m$. The last given data are exactly the same as those of the Timoshenko beam studied in Ref. [20]. The lowest five natural frequencies, ω_v ($v = 1$–5), of the Timoshenko beam are shown in Table 2, where "Exact" refers to the exact solutions given by Ref. [20], "FEM" refers to the natural frequencies obtained from FEM based on the element stiffness and mass matrices given by Ref. [21]. From Table 2, one sees that the results of LTMM1 are very close to those of FEM or Exact, particularly for the lowest three natural frequencies. For this reason, the corresponding lowest five mode shapes obtained from LTMM1 are also in good agreement with the exact ones given by Ref. [20] as one may see from Figs. 3(a) and (b). Where the legends for the curves are similar to those for the curves shown in Figs. 2(a) and (b). Note that the element mass matrix of FEM given by Ref. [21] is derived from the *distributed-mass* model and the formulation of LTMM1 is based on the *lumped-mass* model, this will be one of the main reasons that, in Table 2, the FEM results are closer to the exact solution than the LTMM1 results. In general, reducing the size of each beam segment will improve the accuracy of the LTMM1 results.

4.1.2. A uniform beam carrying various concentrated elements

Figs. 4(a)–(c) show the examples for a uniform beam carrying various concentrated elements [8,9,12]. Among which, Fig. 4(a) shows a uniform cantilever beam carrying an intermediate translational spring $k_{t,i}$ and a rotational spring $k_{r,i}$ located at the position $x = x_i$ [9,12]. The beam shown in Fig. 4(b) is the same as that shown in Fig. 4(a), except that an additional elastic-support lumped mass m_{n+1} is attached to the free (right) end of the beam with the stiffness constant of the translational spring being $k_{t,n+1}$ [12]. Fig. 4(c) shows a beam with its left end spring-hinged, right end carrying an eccentric lumped mass m_{n+1} with eccentricity e_{n+1} and also constrained by an intermediate translational spring $k_{t,i}$ and a rotational spring $k_{r,i}$ [12]. It is evident that Figs. 4(a)–(c) are the special cases of Fig. 4(d), where each of station Nos. 1, i and $n+1$ is attached by three kinds of concentrated elements as shown in Fig. 1(a), but the eccentricities of m_1 and m_i are zero, and that of

Table 2
The lowest five natural frequencies, ω_v ($v = 1-5$), for a Timoshenko beam obtained from LTMM1, FEM and exact solutions

Boundary conditions	Methods	Natural frequencies, ω_v (rad/s)				
		ω_1	ω_2	ω_3	ω_4	ω_5
P–P	LTMM1[a]	121.1135	431.7565	844.6955	1304.1615	1782.9015
	FEM[b]	121.1160	431.8731	845.5643	1307.3538	1791.0850
	Exact [18]	121.1227	432.1613	847.6788	1315.0820	1810.8499
C–C	LTMM1	242.4285	570.4705	965.9705	1395.0525	1844.8265
	FEM	242.4485	570.7416	967.2862	1398.9924	1853.9050
	Exact [18]	242.5021	571.4142	970.4942	1408.5430	1875.8482
C–F	LTMM1	44.2085	245.8105	599.5665	1014.8815	1462.6305
	FEM	44.2119	245.8795	600.0248	1016.6415	1467.4427
	Exact [18]	44.2123	245.9332	600.7741	1020.1952	1477.9447

[a]Total number of beam segments (or fields) is $n = 40$.
[b]Total number of beam elements is $n_e = 40$.

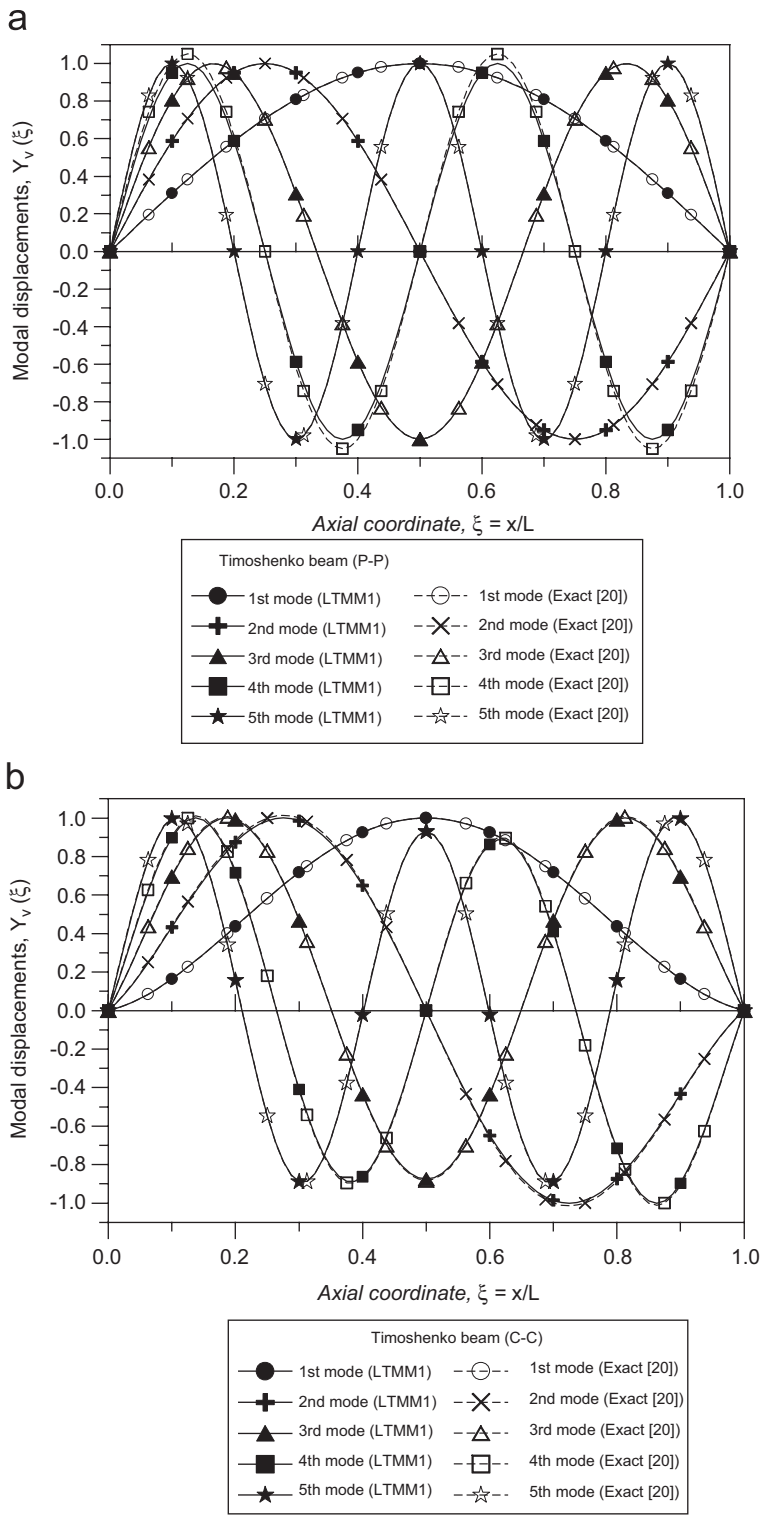

Fig. 3. The lowest five mode shapes of the uniform *Timoshenko beam* corresponding to the natural frequencies (ω_v) listed in Table 2: (a) P–P beam; (b) C–C beam: —●—, —+—, —▲—, —■—, —⋆— obtained from LTMM1; ---○---, ---×---, ---△---, ---□---, ---☆--- obtained from exact solutions [20].

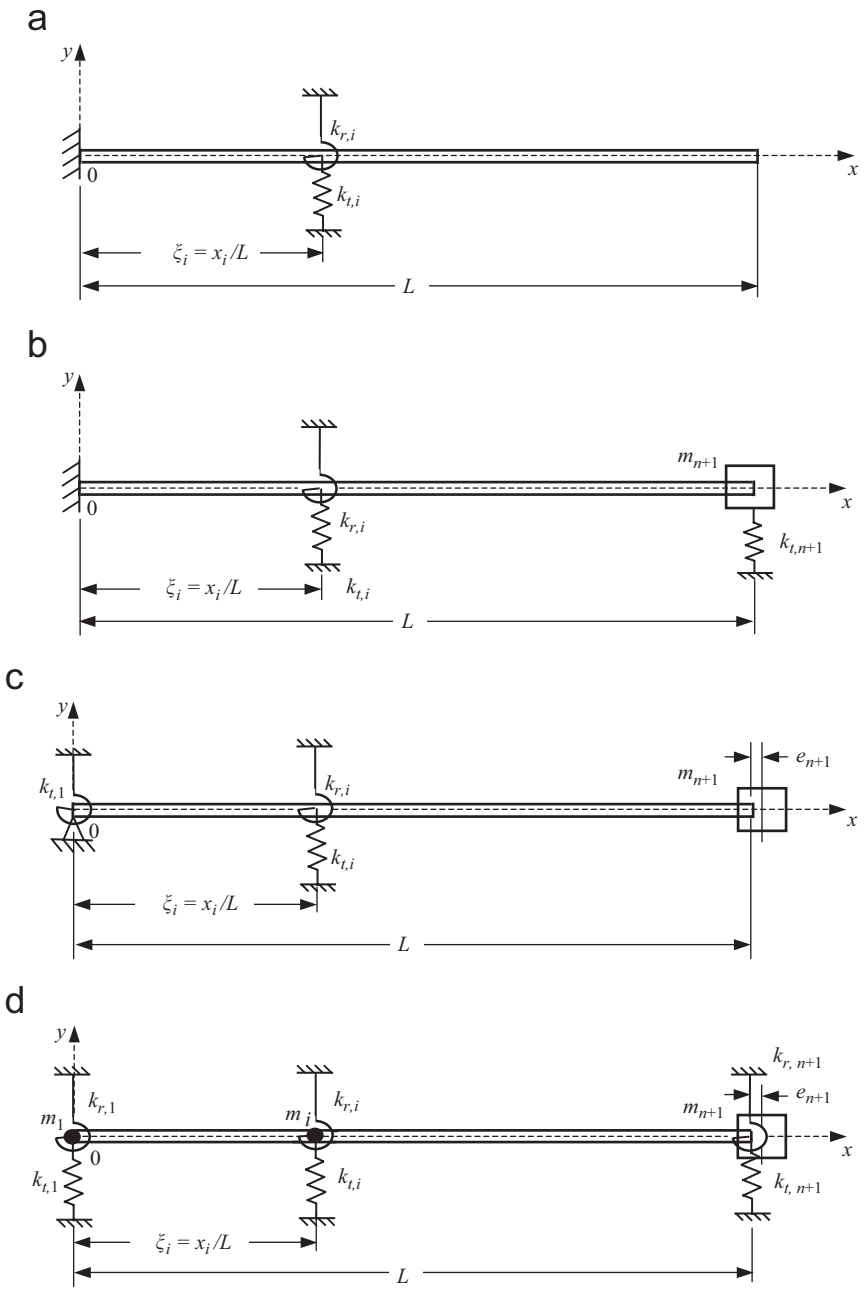

Fig. 4. (a) A cantilever beam with in-span elastic constraints; (b) a cantilever beam with in-span elastic constraints and carrying an elastic-support tip mass; (c) a spring-hinged beam with in-span elastic constraints and carrying an eccentric tip mass; (d) a uniform F–F beam carrying three kinds of concentrated elements (lumped masses m_i, translational springs $k_{t,i}$ and rotational springs $k_{r,i}$).

m_{n+1} is e_{n+1}. It is evident that, if one sets $k_{t,1} = k_{r,1} = \infty$, $m_1 = 0$, $k_{t,n+1} = k_{r,n+1} = 0$, $m_{n+1} = 0$ and $e_{n+1} = 0$ for the beam shown in Fig. 4(d), then one obtains the beam shown in Fig. 4(a).

The dimensions of the beam and its physical properties are the same as those of the uniform Euler–Bernoulli beam studied in the last subsection. The lowest three frequency coefficients, $\beta_v L = [\omega_v^2 \rho A L^4/(EI)]^{1/4}$ ($v = 1-3$), for the beam shown in Fig. 4(a) are listed in Table 3 for the case of $k_{t,i} = 0$ and $k^*_{r,i} = k_{r,i}/\tilde{k}_r = 1, 10, 100$ with reference stiffness constant for the rotational spring $\tilde{k}_r = E_1 I_1/L = 4.1112 \times 10^3$ N m

Table 3
The lowest three frequency coefficients, $\beta_v L = [\omega_v^2 \rho A L^4/(EI)]^{1/4}$ ($v = 1$–3), for the cantilever beam with elastic constraints at $\xi_i = x_i/L$ as shown in Fig. 4(a) with $k_{t,i}^* = 0$, ($k_{r,i} = 1$, 10, 100) and ($\xi = 0.2, 0.8$)

$\xi_i = x_i/L$	$k_{r,i}^* = k_{r,i}/\tilde{k}_r$	Methods	Frequency coefficients, $\beta_v L = [\omega_v^2 \rho A L^4/(EI)]^{1/4}$		
			$\beta_1 L$	$\beta_2 L$	$\beta_3 L$
0.2	1	LTMM1	1.9247	4.7409	7.8679
		Ref. [9]	1.9247	4.7437	7.8744
		Ref. [12]	1.9247	4.7437	7.8744
	10	LTMM1	2.1248	5.0353	8.0100
		Ref. [9]	2.3018	5.5258	8.4162
		Ref. [12]	2.1253	5.0375	8.0159
	100	LTMM1	2.3009	5.5225	8.4105
		Ref. [9]	2.3377	5.6753	8.6159
		Ref. [12]	2.3014	5.5258	8.4162
0.8	1	LTMM1	2.0728	4.8535	7.8937
		Ref. [9]	2.0740	4.8564	7.9005
		Ref. [12]	2.0740	4.8564	7.9005
	10	LTMM1	2.4497	5.5879	8.2446
		Ref. [9]	2.4503	5.5904	8.2544
		Ref. [12]	2.4503	5.5904	8.2544
	100	LTMM1	2.5919	6.2539	9.2271
		Ref. [9]	2.5916	6.2550	9.2425
		Ref. [12]	2.5916	6.2550	9.2425

as has been defined at the beginning of this Section 4. The location of the in-span rotational spring is at $\xi_i = x_i/L = 0.2$ and 0.8, respectively.

From Table 3, one sees that the results of the LTMM1 are very close to the corresponding ones obtained from the traditional analytical methods given by the Refs. [9,12]. Besides, Table 3 reveals that (i) the natural frequencies of the beam increase with the increase of rotational spring stiffness ($k_{r,i}$ or $k_{r,i}^*$) if its distance from the clamped end ($\xi_i = x_i/L$) is constant and (ii) the natural frequencies of the beam increase with the increase of distance from the clamped end ($\xi_i = x_i/L$) if the rotational stiffness ($k_{r,i}$ or $k_{r,i}^*$) is constant. Note that, in Table 3, the results of Refs. [9,12] are close to each other while the LTMM1 results are relatively far from the last results, this is because the results of Refs. [9,12] are based on the *exact* closed form solution of the beam equation while the results of the LTMM1 are the *approximate* ones. In general, one can improve the accuracy of the LTMM1 results by reducing the size of each beam segment.

For the cantilever beam with in-span constraint and carrying an elastic-support tip mass as shown in Fig. 4(b), Table 4 lists its lowest frequency coefficient ($\beta_1 L$) for the case of no in-span constraint (i.e., $k_{t,i} = k_{r,i} = 0$), and the case of ($k_{t,n+1}^* = k_{t,n+1}/\tilde{k}_t = 0, 10$) and ($m_{n+1}^* = m_{n+1}/\tilde{m} = 0, 0.2, 0.6, 8$). From Table 4, one sees that the results of LTMM1 are also very close to those of Refs. [8,12].

For the spring-hinged (with rotational stiffness constant $k_{r,1}$) beam with in-span constraint (with stiffness constants $k_{t,i}$ and $k_{r,i}$) and carrying an eccentric tip mass (m_{n+1} and e_{n+1}) shown in Fig. 4(c), the influence of the attachments ($k_{r,1}$, $k_{r,i}$, $k_{t,i}$, J_{n+1}, e_{n+1} and ξ_i) on the lowest five frequency coefficients are listed in Table 5. It is evident that, for all the cases studied, the results of LTMM1 are in good agreement with those of Ref. [12].

Based on the excellent agreement between the numerical results of the LTMM1 (or LTMM0) and the corresponding ones of the analytical methods given by the existing literature as shown in Tables 1–5, one may believe that the presented theory and the developed computer program for this paper should be reliable.

4.2. A uniform beam with overhang and carrying multiple concentrated elements

Fig. 5 shows a uniform Euler–Bernoulli P–P beam (diameter $d = d_1 = 0.03$ m and total length $L = 2.0$ m) with overhang and carrying three identical sets of concentrated elements. Each set of concentrated elements

Table 4
The lowest frequency coefficient ($\beta_1 L$) for a cantilever beam with in-span constraint and carrying an elastic-support tip mass (cf. Fig. 4(b)) with $k^*_{t,i} = k^*_{r,i} = 0$, ($k^*_{t,n+1} = 0, 10$) and ($m^*_{n+1} = 0, 0.2, 0.6, 8$)

$k^*_{t,n+1} = k_{t,n+1}/\tilde{k}_t$	$m^*_{n+1} = m_{n+1}/\tilde{m}$	Methods	$\beta_1 L$
0	0	LTMM1	1.8755
		Ref. [8]	1.8751
	0.2	LTMM1	1.6166
		Ref. [8]	1.6164
	0.6	LTMM1	1.3771
		Ref. [8]	1.3757
	8	LTMM1	0.7797
		Ref. [8]	—
10	0	LTMM1	2.6395
		Ref. [12]	2.6389
	0.2	LTMM1	2.3144
		Ref. [12]	2.3144
	0.6	LTMM1	1.9806
		Ref. [12]	1.9808
	8	LTMM1	1.1190
		Ref. [12]	1.1209

Table 5
Influence of the parameters $k^*_{r,1}$, $k^*_{r,i}$, $k^*_{t,i}$, J^*_{n+1}, e^*_{n+1} and ξ_i on the lowest five frequency coefficients, $\beta_v L = [\omega_v^2 \rho A L^4/(EI)]^{1/4}$ ($v = 1-5$), of the spring-hinged beam with in-span constraint and carrying an elastic-support eccentric tip mass shown in Fig. 4(c) with $m^*_{n+1} = m_{n+1}/\tilde{m} = 5$

$k^*_{r,1}$	$k^*_{r,i}$	$k^*_{t,i}$	J^*_{n+1}	e^*_{n+1}	ξ_i	Methods	Frequency coefficients, $\beta_v L = [\omega_v^2 \rho A L^4/(EI)]^{1/4}$				
							$\beta_1 L$	$\beta_2 L$	$\beta_3 L$	$\beta_4 L$	$\beta_5 L$
0	0	10	0	0	0.4	LTMM1	0.7096	3.3034	6.3056	9.4373	12.5765
						Ref. [12]	0.7096	3.3034	6.3057	9.4373	12.5765
0	10	10	0	0	0.4	LTMM1	1.0354	3.3738	6.6382	9.7096	12.6079
						Ref. [12]	1.0354	3.3738	6.6382	9.7096	12.6080
0.1	10	10	0	0	0.5	LTMM1	1.0963	3.3293	6.8280	9.4464	12.8998
						Ref. [12]	1.0964	3.3293	6.8281	9.4465	12.8998
10^5	10	10	1	0.1	0.5	LTMM1	0.9590	1.8018	4.8435	8.3546	11.0203
						Ref. [12]	0.9591	1.8018	4.8435	8.3546	11.0203

Note: $k^*_{r,1} = \dfrac{k_{r,1}}{\tilde{k}_r}$, $k^*_{r,i} = \dfrac{k_{r,i}}{\tilde{k}_r}$, $k^*_{t,i} = \dfrac{k_{t,i}}{\tilde{k}_t}$, $J^*_{n+1} = \dfrac{J_{n+1}}{\tilde{J}}$, $e^*_{n+1} = \dfrac{e_{n+1}}{L}$, $\xi_i = \dfrac{x_i}{L}$.

includes a lumped mass m_i (with rotary inertia J_i and eccentricity e_i), a translational spring (with stiffness constant $k_{t,i}$) and a rotational spring (with stiffness constant $k_{r,i}$). The magnitudes of the concentrated elements are: $m_i = \tilde{m} = 11.09833\,\text{kg}$, $J_i = 0.1\tilde{J} = 4.439332\,\text{kg m}^2$, $e_i = 0.01L = 0.02\,\text{m}$, $k_{t,i} = \tilde{k}_t = 1.0278 \times 10^3\,\text{N/m}$ and $k_{r,i} = \tilde{k}_r = 4.1112 \times 10^3\,\text{N m}$ (for $i = 6, 21, 36$), where i denotes the station numbering and the total number of stations is $n + 1 = 41$. The digits in Fig. 5 represent the numberings for the associated stations, and the locations of the three sets of concentrated elements are: $\xi_i = x_i/L = 0.125, 0.5$ and 0.875 (for $i = 6, 21, 36$), respectively. It is noted that the unit for all lengths in the figure is "meter".

The lowest five natural frequencies of the beam, ω_v ($v = 1$–5), are shown in Table 6. For comparisons, the corresponding ones obtained from FEM and those for the same beam without any attachments are also listed in Table 6. From the table one sees that the values of ω_v ($v = 1$–5) obtained from LTMM1 are very close to those obtained from FEM, beside, the three sets of attachments significantly reduce the lowest five natural frequencies of the uniform P–P beam with overhang.

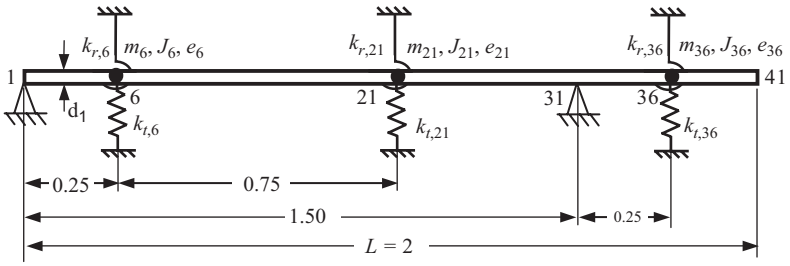

Fig. 5. A uniform Euler–Bernoulli P–P beam (diameter $d_1 = 0.03\,\text{m}$) with "overhang" and carrying three identical sets of concentrated elements. Each set of attachments includes a lumped mass m_i (with rotary inertia J_i and eccentricity e_i), a translational spring $k_{t,i}$ and a rotational spring $k_{r,i}$, located at station Nos. 6, 21 and 36 (i.e., $i = 6, 21$ and 36), respectively. The magnitudes of the elements are: $m_i = \tilde{m} = 11.09833\,\text{kg}$, $J_i = 0.1\tilde{J} = 4.439332\,\text{kg m}^2$, $e_i = 0.01L = 0.02\,\text{m}$, $k_{t,i} = \tilde{k}_t = 1.0278 \times 10^3\,\text{N/m}$ and $k_{r,i} = \tilde{k}_r = 4.1112 \times 10^3\,\text{N m}$. (The unit for all the lengths in the figure is "meter".)

Table 6
The lowest five natural frequencies, ω_v ($v = 1$–5), for the uniform Euler–Bernoulli P–P beam with "overhang" and carrying three identical sets of concentrated elements located at station Nos. 6, 21 and 36 (i.e., $i = 6, 21$ and 36), respectively, as shown in Fig. 5

Loading conditions	Methods	Natural frequencies, ω_v (rad/s)				
		ω_1	ω_2	ω_3	ω_4	ω_5
$m_i, J_i, e_i, k_{t,i}$ and $k_{r,i}$	LTMM1	47.8632	80.1400	168.9607	227.9254	396.5510
	FEM	47.8667	80.1423	168.9607	227.9248	396.5531
No attachments	LTMM1	147.8154	364.3721	797.8556	1621.5400	2555.4001
	FEM	147.9235	365.1628	798.3614	1623.0366	2584.6892

Note: $m_i = J_i = e_i = k_{t,i} = k_{r,i} = 0$ for $i = 1$–41 except those with $i = 6, 21$ and 36.

It is noted that, for the beam showing in Fig. 5, an additional effort must be paid if the classical LTMM0 is used to determine its natural frequencies because of the existence of the intermediate rigid support (at station No. 31), however, this is not true for the presented LTMM1.

4.3. A "stepped" beam carrying multiple sets of concentrated elements

The purpose of this subsection is to study the availability of the presented LTMM1 for the free vibration analysis of the non-uniform beams. All conditions of the current stepped P–P beam are the same as the uniform beam with overhang studied in the last subsection (cf. Fig. 5) except that the intermediate rigid support at station No. 31 is moved to the right end of the beam (at station No. 41) and there exists two step changes in cross-sections with diameters of the stepped beam segments to be $d_1 = 0.03\,\text{m}$, $d_2 = 0.04\,\text{m}$ and $d_3 = 0.05\,\text{m}$, as one may see from Fig. 6. The lowest five natural frequencies of the stepped beam, ω_v ($v = 1$–5), obtained from LTMM1 and FEM are listed in Table 7(a) for the Euler–Bernoulli beam and in Table 7(b) for the Timoshenko beam. In each table, six cases are studied: In *Case* 1, the magnitudes of all the attachments are equal to zero except the three lumped masses ($m_6 = m_{21} = m_{36} = 11.09833\,\text{kg}$) located at station Nos. 6, 21 and 36, respectively, without eccentricities (i.e., $e_6 = e_{21} = e_{36} = 0$). In *Case* 2, all conditions are the same as *Case* 1 except that the three rotary inertias ($J_6 = J_{21} = J_{36} = 4.439332\,\text{kg m}^2$) of the three lumped masses are considered. In *Case* 3, all conditions are the same as *Case* 2 except that the eccentricities ($e_6 = e_{21} = e_{36} = 0.02\,\text{m}$) of the three lumped masses are also considered. In *Case* 4, all conditions are the same as *Case* 2 but the three lumped masses together with their rotary inertias are replaced by three identical translational springs ($k_{t,6} = k_{t,21} = k_{t,36} = \tilde{k}_t = 1.0278 \times 10^3\,\text{N/m}$) together with three identical rotational springs ($k_{r,6} = k_{r,21} = k_{r,36} = \tilde{k}_r = 4.1112 \times 10^3\,\text{N m}$). In *Case* 5, all the three sets of concentrated elements (including the effect of eccentricities) are considered. In the final *Case* 6, the P–P beam without any attachment is studied.

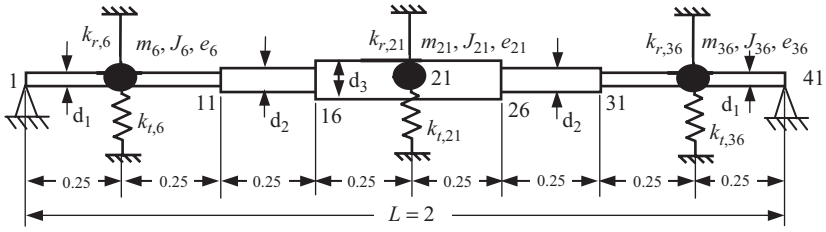

Fig. 6. A three-step P–P beam carrying three identical sets of concentrated elements. Each set of attachments includes a lumped mass m_i (with rotary inertia J_i and eccentricity e_i), a translational spring $k_{t,i}$ and a rotational spring $k_{r,i}$, located at station Nos. 6, 21 and 36 (i.e., $i = 6, 21, 36$), respectively. The magnitudes of the elements are: $m_i = \tilde{m} = 11.09833\,\text{kg}$, $J_i = 0.1\tilde{J} = 4.439332\,\text{kg m}^2$, $e_i = 0.01L = 0.02\,\text{m}$, $k_{t,i} = \tilde{k}_t = 1.0278 \times 10^3\,\text{N/m}$ and $k_{r,i} = \tilde{k}_r = 4.1112 \times 10^3\,\text{N m}$. The diameters of the three stepped beam segments are: $d_1 = 0.03\,\text{m}$, $d_2 = 0.04\,\text{m}$, $d_3 = 0.05\,\text{m}$. (The unit for all the lengths in the figure is "meter".)

Table 7
The lowest five natural frequencies, ω_v ($v = 1$–5), for the three-step P–P beam carrying three identical sets of concentrated elements located at station Nos. 6, 21 and 36 (i.e., $i = 6, 21$ and 36), respectively, as shown in Fig. 6

Cases	Loading conditions	Methods	Natural frequencies, ω_r (rad/s)				
			ω_1	ω_2	ω_3	ω_4	ω_5
(a) For Euler–Bernoulli beam							
1	m_i only	LTMM1	74.9470	229.3248	460.0856	1153.3536	2023.0598
		FEM	74.9429	229.3712	460.0933	1153.5451	2024.3200
2	m_i and J_i	LTMM1	52.7337	104.4908	268.8823	279.4975	468.0654
	(no eccentricities)	FEM	52.7324	104.4947	268.8604	279.5016	468.0792
3	m_i, J_i and e_i	LTMM1	52.7189	104.4501	268.0518	280.2568	467.2115
		FEM	52.7176	104.4539	268.0319	280.2588	467.2283
4	$k_{t,i}$ and $k_{r,i}$ only	LTMM1	121.6619	414.0007	1100.3243	1866.7750	2900.6343
		FEM	121.6459	414.2661	1100.9683	1867.2391	2900.7577
5	m_i, J_i, e_i,	LTMM1	57.3317	108.1611	268.9405	281.6411	467.3322
	$k_{t,i}$ and $k_{r,i}$	FEM	57.3303	108.1651	268.9206	281.6434	467.3489
6	No attachments	LTMM1	108.0544	402.7993	973.7171	1861.8415	2662.7367
		FEDM	108.0434	403.0264	974.9014	1862.0029	2666.4724
Note: $m_i = J_i = e_i = k_{t,i} = k_{r,i} = 0$ for $i = 1$–41 except those with $i = 6, 21$ and 36.							
(b) For Timoshenko beam							
1	m_i only	LTMM1	74.8984	228.9752	458.1580	1144.7258	1998.9980
		FEM	74.8942	229.0217	458.1680	1144.9611	2000.4430
2	m_i and J_i	LTMM1	52.7254	104.4760	267.7368	278.2624	466.0457
	(no eccentricities)	FEM	52.7242	104.4799	267.7156	278.2669	466.0619
3	m_i, J_i and e_i	LTMM1	52.7106	104.4353	266.9065	279.0217	465.2039
		FEM	52.7094	104.4392	266.8873	279.0242	465.2230
4	$k_{t,i}$ and $k_{r,i}$ only	LTMM1	121.5682	413.2632	1095.4202	1852.5828	2866.6001
		FEM	121.5522	413.5294	1096.0910	1853.2121	2867.3548
5	m_i, J_i, e_i,	LTMM1	57.3213	108.1464	267.7999	280.4112	465.3248
	$k_{t,i}$ and $k_{r,i}$		(−0.0181%)	(−0.0136%)	(−0.4241%)	(−0.4367%)	(−0.4295%)
		FEM	57.3199	108.1505	267.7806	280.4138	465.3437
6	No attachments	LTMM1	107.9888	402.1009	970.0299	1847.1258	2634.5980
		FEM	107.9779	402.3287	971.2252	1847.4502	2638.7199

Note: (i) $m_i = J_i = e_i = k_{t,i} = k_{r,i} = 0$ for $i = 1$–41 except those with $i = 6, 21$ and 36.
$\varepsilon_v\% = (\omega_{v\text{Timosh}} - \omega_{v\text{Euler}}) \times 100\%/\omega_{v\text{Euler}}$, $v = 1$–5, with $\omega_{v\text{Timosh}}$ and $\omega_{v\text{Euler}}$ denoting the vth natural frequencies of the Timoshenko beam and Euler–Bernoulli beam, respectively.

From Tables 7(a) and (b) one finds that the lowest five natural frequencies of the Timoshenko beam are only slightly smaller than the corresponding ones of the Euler–Bernoulli beam, because the slenderness ratio of the current P–P beam is small. For convenience of comparison, the reducing rates of the lowest five natural frequencies of the Timoshenko beam in the loading condition of *Case* 5 ($\omega_{1\text{Timosh}}$ to $\omega_{5\text{Timosh}}$) with respect to

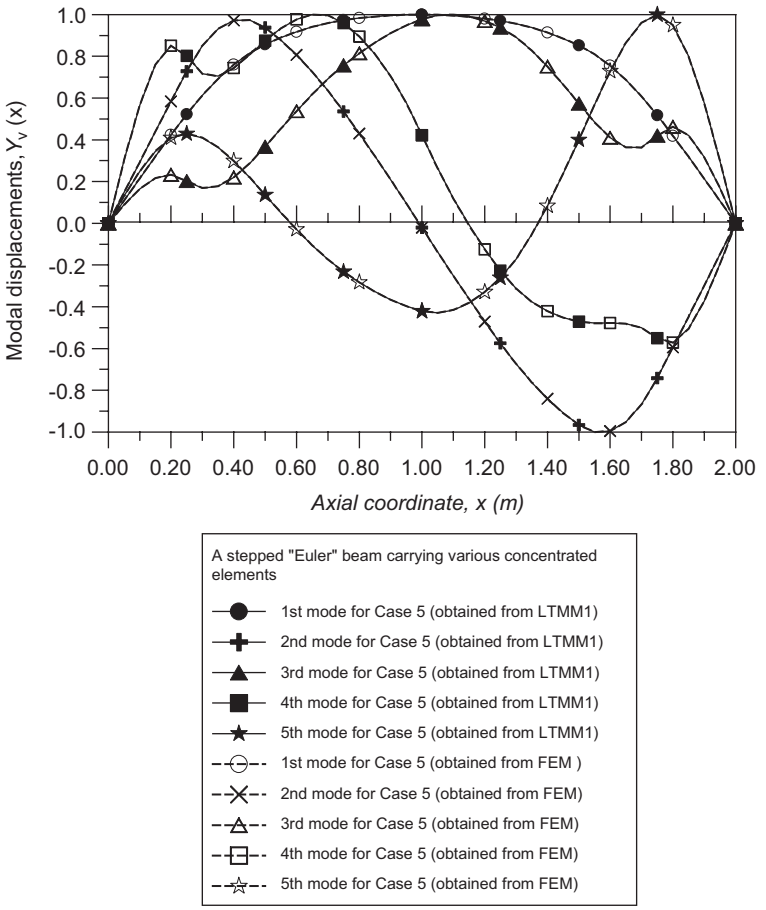

Fig. 7. The lowest five mode shapes of the "stepped" Euler–Bernoulli beam carrying three identical sets of concentrated elements located at station Nos. 6, 21 and 36, respectively, as shown in Fig. 6: —●—, —+—, —▲—, —■—, —⋆— obtained from LTMM1; ---◯---, ---×---, ---△---, ---□---, ---☆--- obtained from FEM.

the corresponding ones of the Euler–Bernoulli beam ($\omega_{1\text{Euler}}$ to $\omega_{5\text{Euler}}$) are listed in the parentheses (.) of Table 7(b). They are calculated from the formula: $\varepsilon_v\% = (\omega_{v\text{Timosh}} - \omega_{v\text{Euler}}) \times 100\%/\omega_{v\text{Euler}}$. It is evident that the percentage difference increases with the vibration modes. In Tables 7(a) and (b) the natural frequencies associated with the last percentage differences are underlined.

The lowest five mode shapes of the Euler–Bernoulli beam in loading condition of *Case* 5 are shown in Fig. 7. Where the curves (—●—, —+—, —▲—, —■—, —⋆—) are obtained from LTMM1 and those (---◯---, ---×---, ---△---, ---□---, ---☆---) from FEM with the symbols ● (or ◯), + (or ×), ▲ (or △), ■ (or □) and ⋆ (or ☆) denoting the 1st, 2nd, 3rd, 4th and 5th mode shapes, respectively. Because the agreement between the lowest five natural frequencies obtained from LTMM1 and the corresponding ones from FEM is excellent as shown in Table 7(a), so is the corresponding lowest five mode shapes shown in Fig. 7. It has been found that the last conclusion for the mode shapes of Euler–Bernoulli beam is also available for the lowest five mode shapes of the Timoshenko beam with its lowest five natural frequencies shown in Table 7(b).

5. Conclusions

1. Based on the formulation for a "free–free" beam carying a number of sets of concentrated elements with each set consisting of a lumped mass (with or without rotary inertia and/or eccentricity), a translational spring and a rotational spring, one may easily determine the lowest several natural frequencies and the corresponding mode shapes of a uniform or non-uniform beam with either classical or non-classical

boundary conditions by using the LTMM1 presented in this paper. To achieve the last goal, the only thing that one should do is to adjust the magnitudes of the stiffness constants of the translational spring and/or the rotational spring attached to each station together with the magnitudes of the cross-sectional area and length of the relevant beam segment.

2. In most of the existing LTMM0, the shear deformation and rotary inertia of the beam segments and the eccentricities of the attached lumped masses are neglected, but all of these factors have been considered in the formulation of LTMM1. Therefore, most of the problems studied in the existing literature concerned can be easily solved with the presented LTMM1.

Appendix. Frequency equations and initial parameters for the "classical" LTMM0

Following the similar steps of arriving at the frequency equation (32) and the initial parameters given by Eq. (33) for a "free–free" (F–F) beam, one may obtain the corresponding ones for the pinned–pinned (P–P), clamped–clamped (C–C), clamped–free (C–F) and clamped–pinned (C–P) beams from their boundary conditions and Eq. (28), respectively:

(i) For the P–P beam

$$\Delta(\omega) = \begin{vmatrix} \overline{T}_{12} & \overline{T}_{14} \\ \overline{T}_{32} & \overline{T}_{34} \end{vmatrix} = 0, \tag{A.1a}$$

$$\{\delta\}_0 = [0 \;\; 1 \;\; 0 \;\; -\overline{T}_{12}/\overline{T}_{14}]^{\mathrm{T}}. \tag{A.1b}$$

(ii) For the C–C beam

$$\Delta(\omega) = \begin{vmatrix} \overline{T}_{13} & \overline{T}_{14} \\ \overline{T}_{23} & \overline{T}_{24} \end{vmatrix} = 0, \tag{A.2a}$$

$$\{\delta\}_0 = [0 \;\; 0 \;\; 1 \;\; -\overline{T}_{13}/\overline{T}_{14}]^{\mathrm{T}}. \tag{A.2b}$$

(iii) For the C–F beam

$$\Delta(\omega) = \begin{vmatrix} \overline{T}_{33} & \overline{T}_{34} \\ \overline{T}_{43} & \overline{T}_{44} \end{vmatrix} = 0, \tag{A.3a}$$

$$\{\delta\}_0 = [0 \;\; 0 \;\; 1 \;\; -\overline{T}_{33}/\overline{T}_{34}]^{\mathrm{T}}. \tag{A.3b}$$

(iv) For the C–P beam

$$\Delta(\omega) = \begin{vmatrix} \overline{T}_{13} & \overline{T}_{14} \\ \overline{T}_{33} & \overline{T}_{34} \end{vmatrix} = 0, \tag{A.4a}$$

$$\{\delta\}_0 = [0 \;\; 0 \;\; 1 \;\; -\overline{T}_{13}/\overline{T}_{14}]^{\mathrm{T}}. \tag{A.4b}$$

References

[1] N.O. Myklestad, A new method of calculating normal modes of uncoupled bending vibration of airplane wings and other types of beams, *Journal of the Aeronautical Science* 11 (1944) 153–162.
[2] M.A. Prohl, A general method for calculating critical speeds of flexible rotors, *Journal of Applied Mechanics* 12 (1945) 142–148.
[3] L. Meirovitch, *Analytical Methods in Vibrations*, Macmillan, London, 1967.
[4] W.D. Pilkey, P.Y. Chang, *Modern Formulas for Statics and Dynamics*, McGraw-Hill, New York, 1978.
[5] M.J. Maurizi, R.E. Rossi, J.A. Reyes, Vibration frequencies for a uniform beam with one end spring-hinged and subjected to a translational restraint at the other end, *Journal of Sound and Vibration* 48 (4) (1976) 565–568.

[6] A. Rutenberg, Vibration frequencies for a uniform cantilever with a rotational constraint at a point, American Society of Mechanical Engineers, *Journal of Applied Mechanics* 45 (1978) 422–423.
[7] K. Takahashi, Eigenvalue problem of a beam with a mass and spring at the end subjected to an axial force, *Journal of Sound and Vibration* 71 (3) (1980) 453–457.
[8] N.G. Stephen, Vibration of a cantilevered beam carrying a tip heavy body by Dunkerley's method, *Journal of Sound and Vibration* 70 (3) (1980) 463–465.
[9] J.H. Lau, Vibration frequencies and mode shapes for a constrained cantilever, American Society of Mechanical Engineers, *Journal of Applied Mechanics* 51 (1984) 182–187.
[10] M. Gurgoze, A note on the vibrations of restrained beams and rods with point masses, *Journal of Sound and Vibration* 96 (4) (1984) 461–468.
[11] M. Gurgoze, On the vibrations of restrained beams and rods with heavy masses, *Journal of Sound and Vibration* 100 (4) (1985) 588–589.
[12] W.H. Liu, C.C. Huang, Vibrations of a constrained beam carrying a heavy tip body, *Journal of Sound and Vibration* 123 (1) (1988) 15–29.
[13] C.N. Bapat, C. Bapat, Natural frequencies of a beam with non-classical boundary conditions and concentrated masses, *Journal of Sound and Vibration* 112 (1) (1987) 117–182.
[14] M. Geradin, S.L. Chen, An exact model reduction technique for beam structures: combination of transfer and dynamic stiffness matrices, *Journal of Sound and Vibration* 185 (3) (1995) 431–440.
[15] M. Aleyaasin, M. Ebrahimi, R. Whalley, Vibration analysis of distributed-lumped rotor systems, *Computer Methods in Applied Mechanics and Engineering* 189 (2000) 545–558.
[16] J.S. Wu, P.Y. Shih, The dynamic analysis of a multispan fluid-conveying pipe subjected to external load, *Journal of Sound and Vibration* 239 (2) (2001) 201–215.
[17] J.S. Wu, C.W. Dai, Dynamic responses of multispan non-uniform beam due to moving loads, *Journal of Structural Engineering, ASCE* 113 (3) (1987) 458–474.
[18] M.F. Spotts, *Design of Machine Elements*, fourth ed., Prentice-Hall Inc., Englewood Cliffs, NJ, 1978.
[19] S. Timoshenko, D.H. Young, W. Weaver Jr., *Vibration Problems in Engineering*, fourth ed., Wiley, New York, 1974.
[20] J.S. Wu, D.W. Chen, Free vibration analysis of a Timoshenko beam carrying multiple spring-mass systems by using the numerical assembly technique, *International Journal for Numerical Methods in Engineering* 50 (2001) 1039–1058.
[21] J.S. Przemieniecki, *Theory of Matrix Structural Analysis*, McGraw-Hill, New York, 1968.